Electron correlations in single-electron capture from heliumlike atomic systems

Ivan Mančev
Department of Physics, University of Niš, P.O. Box 91, 18001 Niš, Yugoslavia
(Received 20 October 1998)

Total cross sections for single-electron transfer from two selected heliumlike atomic systems by bare projectiles are computed by means of the four-body continuum distorted-wave approximation. The effect of dynamic electron correlations is explicitly taken into account through the complete perturbation potentials. Specifically, we consider the symmetric He^{2+}-He and asymmetric H^+-Li^+ collisions in a large energy range from 50 to 10 000 keV. With regard to a previous work of Belkić *et al.* [Phys. Rev. A **56**, 3675 (1997)], where a major influence of electronic correlations on single-electron capture by fast protons in helium was found, the present paper expands the study to higher projectile (He^{2+}) and target (Li^+) nuclear charges, with the purpose of determining whether electronic correlations remain important. The *prior* and *post* total cross sections are found to be in satisfactory agreement with the available experimental data. [S1050-2947(99)04707-1]

PACS number(s): 34.70.+e, 82.30.Fi

I. INTRODUCTION

The three-body continuum distorted-wave (CDW-3B) method (with the original accronym CDW) [1–5] is one of the most adequate approximations for treating charge exchange in fast ion-atom collisions. In the case of two-electron transitions, the CDW-IPM and CDW-IEM approximations were used in Refs. [6,7] and [8,9], respectively. IPM refers to the independent particle model and IEM refers to the independent event model. During the last few years, much attention has been paid to developing an appropriate framework for four-body continuum distorted wave (CDW-4B) models with the primary purpose of describing two-electron transitions at intermediate and high impact energies. Such a full quantum-mechanical CDW-4B method for two-electron capture from heliumlike atomic systems by bare projectiles has been introduced in Refs. [10,11]. The obtained results for formation of H^- in H^+-He collisions were in excellent agreement with the pertinent experimental data. Subsequently, the CDW-4B approximation for double-electron capture was used for other collision systems encompassing some singly and doubly excited final states [12]. Another version of the CDW-4B method with certain additional approximations in perturbation potentials was utilized in Refs. [13–15] to examine simultaneous transfer and excitation, such as: $Si^{15+}+H(1s)\rightarrow Si^{14+}(nl,n'l')+H^+$ and $He^+(1s)+He(1s^2)\rightarrow He(nl,n'l')+He^+(1s)$. Moreover, simultaneous transfer and ionization has also been successfully devised by the CDW-4B model [16]. In addition to these two electron transitions, the CDW-4B approximation has recently been employed in Ref. [17] for the description of single-electron capture. The computed total cross sections for H^+-He collisions were in excellent agreement with available experimental data above 100 keV.

In this work we shall apply the CDW-4B method from Ref. [17] to study single charge exchange:

$$He^{2+}+He\rightarrow He^+ + He^+, \tag{1.1}$$

$$p+Li^+\rightarrow H+Li^{2+}. \tag{1.2}$$

The process (1.1) has previously been treated theoretically by a number of authors. In Refs. [4,5] the prior form of the CDW-3B method was employed with various wave functions for helium. In fact, as pursued further later in Ref. [17], the CDW-4B approximation was adopted in Refs. [4,5] in an initial stage of the study of reaction (1.1). However, the subsequent analysis of Refs. [4,5] was simplified by an additional approximation, yielding an effective three-body transition amplitude containing only one scalar product of the gradient operator as the perturbation. The CDW-IPM was originally introduced in Ref. [6] for double charge exchange and later applied to transfer ionization in Ref. [7]. The CDW-IEM was suggested in Refs. [8,9] and implemented for Eq. (1.1) at energies 100–800 keV/amu. The effect of the static correlation in helium was explicitly taken into account by the use of the Pluvinage wave function, while the dynamic correlation, which originates from the e-e Coulomb interaction during the collision, was ignored. Such a CDW-IEM gave total cross sections that are larger than the available experimental data. The IPM was frequently utilized for calculating the total cross sections for electron capture in He^{2+}-He collisions within various approximations. According to this model, the captured (active) electron is considered as moving in an effective potential V_T, generated by the alpha particle and the passive electron. The IPM and the Roothan-Hartree-Fock target screening were adapted in Ref. [18] within the boundary-corrected first Born (CB1=B1B) perturbation model. The ensuing results were in very good agreement with the measurements. Total cross sections for Eq. (1.1) were also computed by means of the IEM in Refs. [19–21] within the Bassel-Gerjuoy [21] first-order perturbation theory. The coupled channel semiclassical IPM employing a traveling atomic orbital expansion was utilized in Ref. [22] for a description of various one- and two-electron transitions in collisions between fully stripped ions and helium. In Ref. [22], the IPM was applied to two different effective target potentials: $V_T=-1/r-(1+0.4143r)\exp(-2.499r)/r$ and $V_T=-Z_T^{\rm eff}/r$ with effective charge $Z_T^{\rm eff}$. The main drawbacks of the IPM are (i) the dynamic correlation effects are ignored from the onset and (ii) the three-body formalism is used, despite the fact that the considered problems dealt with

two active electrons. Throughout the present paper, the static correlations refer to the effect of the interelectron interaction in an isolated heliumlike atomic system without recourse to its collisions with another particle. Both radial and angular static electron correlations can be taken into account in the IPM through, e.g., configuration interaction (CI) wave functions as accomplished within various models including the CDW-IPM. The dynamic correlations describe the interaction between the two electrons of the hydrogenic systems $(Z_P,e_1)_{f_1}$ and $(Z_T,e_2)_{f_2}$ in the exit channel of the considered single charge exchange, $Z_P+(Z_T;e_1,e_2)_i\rightarrow(Z_P,e_1)_{f_1}+(Z_T,e_2)_{f_2}$, where the parentheses indicate the bound states. This interaction alone is capable of causing a transition of the complex projectile target from an initial to a final state of the entire collisional system. Such a dynamical effect automatically possesses both radial and angular correlations through an inclusion of the interelectronic Coulomb potential $-1/r_{12}=-1/|\vec{r}_1-\vec{r}_2|$ in the final perturbation potential appearing in a post form of the transition amplitude T_{if}^{+}. Here $r_i(i=1,2)$ is the distance of the ith electron from its parent nucleus Z_T of helium.

The classical trajectory Monte Carlo (CTMC) method was employed in Ref. [23] along with a classical model for helium with the two active electrons. The CTMC approach treats all of the participants in a collision (i.e., the projectile, the target nucleus, and two-target electrons) as classical point particles that interact through Coulomb potentials and move according to Newton's law. However, such a model of helium removes the electron-electron force and allows each electron to interact with the target nucleus through a separate Coulomb potential. Hence, the CTMC method cannot provide any information on electron correlation effects.

Thus far, the reaction (1.2) has been theoretically treated in Ref. [24], where the total cross sections were computed in the 50–250 keV energy range by means of the perturbative ''one-and-a-half-centered'' expansion (POHCE) method. Here, the single-particle model was adopted for the target described through a local exponential screening potential of the type $V_T=-2/r-\exp(-3.3954r)/r$. In Ref. [25] an expansion was used in terms of a two-state orthogonal basis set including the so-called ''united atom'' with a charge dependent upon the internuclear distance. Here the IPM was chosen in a way of enabling replacement of the correlation term between the electrons and the Coulomb interactions with the target nucleus Z_T by the model interaction $-Z_T/r_1-Z_T/r_2+1/r_{12}=-Z_T^{\rm eff}/r_1-Z_T^{\rm eff}/r_2$. The wave function of Li^+ ion was a simple product of the hydrogenic orbitals with the effective charge $Z_T^{\rm eff}$. Although the results of Ref. [25] show some improvement over the CTMC approximation [26], both methods completely ignore the dynamic electron correlations. The total cross sections of the CTMC approximation lie above the experimental data of Ref. [27]. The CDW-3B approximation was used to compute the total cross sections in Ref. [28]. The target lithium ion Li^+ was described by several wave functions, but the considered reaction was reduced to a three-body problem. Such a CDW-3B model cannot yield any information about the relative significance of the role of the *dynamic* interelectron interaction in collisions under study.

The contribution from the e-e interaction during the collision to single-electron capture in the He^{2+}-He and H^+-Li^+ scattering has not been previously assessed. Therefore, the main goal of the present work is to search for evidence of dynamic electron correlation effects in these processes with the help of the CDW-4B theory. (Atomic units will be used throughout unless otherwise stated.)

II. THEORY

Reactions (1.1) and (1.2) belong to the following, more general category:

$$Z_P+(Z_T;e_1,e_2)_i\rightarrow(Z_P;e_1)_{f_1}+(Z_T;e_2)_{f_2}, \qquad (2.1)$$

where Z_P and Z_T are nuclear charges of the projectile and target, respectively. The electrons are regarded as distinguishable from each other according to a quantum-mechanical nonrelativistic spin-independent formalism. Let $\vec{s}_{1,2}$ and $\vec{x}_{1,2}$ be the position vectors of the electrons $e_{1,2}$ relative to Z_P and Z_T, respectively. Further, let $\vec{R}=\vec{x}_1-\vec{s}_1=\vec{x}_2-\vec{s}_2$ be the position vector of Z_P with respect to Z_T. We also have $\vec{R}=\vec{\rho}+\vec{Z}$, where $\vec{\rho}$ is the projection of $\vec{R}$ onto the XOY plane and $\vec{Z}$ is the Z component of $\vec{R}$. The vector of the distance between the two electrons is denoted by $\vec{r}_{12}=\vec{x}_1-\vec{x}_2=\vec{s}_1-\vec{s}_2$. The final working expression for the ''reduced'' matrix element of ''prior'' $T^{-}{}_{\rm if}$ and ''post'' $T^{+}{}_{\rm if}$ transition amplitudes $T^{\pm}{}_{\rm if}=R^{\pm}{}_{\rm if}/(2\pi\nu)$ with the *complete* perturbation potentials in the CDW-4B theory is taken from Ref. [17] as

$$R_{if}^{-}=N_{PT}\int\int\int d\vec{R}\,d\vec{x}_1\,d\vec{x}_2 e^{i\vec{A}\cdot\vec{s}_1+i\vec{B}\cdot\vec{x}_1}\varphi_{f_1}^{*}(\vec{s}_1)\varphi_{f_2}^{*}(\vec{x}_2)\,{}_1F_1(i\nu_T;1;i\nu x_1+i\vec{v}\cdot\vec{x}_1)$$
$$\times\left[Z_P\left(\frac{1}{R}-\frac{1}{s_2}\right)\varphi_i(\vec{x}_1,\vec{x}_2)\,{}_1F_1(i\nu_P;1;i\nu s_1+i\vec{v}\cdot\vec{s}_1)-\vec{\nabla}_{x_1}\varphi_i(\vec{x}_1,\vec{x}_1)\cdot\vec{\nabla}_{s_1}\,{}_1F_1(i\nu_P;1;i\nu s_1+i\vec{v}\cdot\vec{s}_1)\right], \qquad (2.2)$$

$$R_{if}^{+}=N_{PT}\int\int\int d\vec{R}\,d\vec{x}_1\,d\vec{x}_2 e^{i\vec{A}\cdot\vec{s}_1+i\vec{B}\cdot\vec{x}_1}\varphi_i(\vec{x}_1,\vec{x}_2)\varphi_{f_2}^{*}(\vec{x}_2)\,{}_1F_1(i\nu_P;1;i\nu s_1+i\vec{v}\cdot\vec{s}_1)$$
$$\times\left\{\left[Z_P\left(\frac{1}{R}-\frac{1}{s_2}\right)+\left(\frac{1}{r_{12}}-\frac{1}{x_1}\right)\right]\varphi_{f_1}^{*}(\vec{s}_1)\,{}_1F_1(i\nu_T;1;i\nu x_1+i\vec{v}\cdot\vec{x}_1)-\vec{\nabla}_{s_1}\varphi_{f_1}^{*}(\vec{s}_1)\cdot\vec{\nabla}_{x_1}\,{}_1F_1(i\nu_T;1;i\nu x_1+i\vec{v}\cdot\vec{x}_1)\right\}. \qquad (2.3)$$

The term reduced is used to denote that, for the purpose of obtaining the total cross sections $Q^{-}_{\rm if}$ and $Q^{+}_{\rm if}$, we have omitted the overall phase factor $\rho^{2iZ_P(Z_T-1)/v}$, which is due to the Coulomb repulsion between Z_P and Z_T-1 in the entrance and exit channels. Here Z_T-1 represents the charge of the screened target nucleus, i.e., of the target core $(Z_T;e_2)$. The symbol ${}_1F_1(a;c;x)$ in Eqs. (2.2) and (2.3) stands for the confluent hypergeometric function, and the wave function of the initial bound state is labeled by $\varphi_i(\vec{x}_1,\vec{x}_2)$. The final bound states of the $(Z_P;e_1)_{f_1}$ and $(Z_T;e_2)_{f_2}$ systems are described by the hydrogen wave functions $\varphi_{f_1}(\vec{s}_1)$ and $\varphi_{f_2}(\vec{x}_2)$, respectively. The quantity N_{PT} is given by $N_{PT}=N^{+}(\nu_P)N^{-*}(\nu_T)$, where $N^{+}(\nu_P)$ and $N^{-}(\nu_T)$ are the Coulomb normalization constants: $N^{\pm}(\nu_K)=\Gamma(1\mp i\nu_K)e^{\pi\nu_K/2}$ $(K=P,T)$, $\nu_P=Z_P/v$, $\nu_T=(Z_T-1)/v$. The momentum transfers $\vec{A}$ and $\vec{B}$ are defined by

$$\vec{\mathcal{B}}=-\vec{\eta}-\left(\frac{v}{2}+\frac{\Delta E}{v}\right)\hat{\vec{v}},\quad \vec{A}=\vec{\eta}-\left(\frac{v}{2}-\frac{\Delta E}{v}\right)\hat{\vec{v}},$$

$$\Delta E=E_i-E_{f_1}-E_{f_2}, \tag{2.4}$$

where E_i and $E_{f_{1,2}}$ are the initial and final binding energies. The vector $\vec{\eta}$ is the transverse momentum transfer: $\vec{\eta}=(\eta\cos\phi_\eta,\eta\sin\phi_\eta 0)$, and the incident velocity vector $\vec{v}$ is chosen as $\vec{v}=(0,0,v)$, so that $\vec{\eta}\cdot\vec{v}=0$. We have assumed a general factorized form for the bound state of the heliumlike target $(Z_T;e_1,e_2)_{1s^2}$:

$$\varphi_i(\vec{x}_1,\vec{x}_2)=\sum_{k,l}\ \varphi_{\alpha k}(\vec{x}_1)\varphi_{\alpha l}(\vec{x}_2), \tag{2.5}$$

where

$$\varphi_{\alpha j}(\vec{r})=N_{\alpha_j}\exp(-\alpha_j r),\quad N_{\alpha_j}=a_j\sqrt{N}\quad (j=k,l), \tag{2.6}$$

with N being the normalization constant. The values of the summation indices k and l, as well as the variationally determined parameters α_j and a_j, depend upon a concrete choice of the wave function.

After the analytical calculations performed via the standard Nordsieck technique, the above expressions for the reduced transition amplitudes become

$$R^{-}_{if}=\mathcal{M}\sum_{k,l}\ N_{\alpha_k}N_{\alpha_l}\left[-\mathcal{U}^{-}_{\nabla}+\frac{Z_P}{2\pi^2}\int\frac{d\vec{\tau}}{\tau^2}(\mathcal{U}_R-\mathcal{U}_{s_2})\right], \tag{2.7}$$

$$R^{+}_{if}=\mathcal{M}\sum_{k,l}\ N_{\alpha_k}N_{\alpha_l}\times\left[-\mathcal{U}^{+}_{\nabla}-\mathcal{U}_{x_1}+\frac{Z_P}{2\pi^2}\int\frac{d\vec{\tau}}{\tau^2}(\mathcal{U}_R-\mathcal{U}_{s_2}+U_{12})\right], \tag{2.8}$$

where $\mathcal{M}=2^9\pi^2(Z_PZ_T)^{3/2}N_{PT}$. The remaining quantities in $R^{\pm}_{\rm if}$ are defined as follows:

$$\mathcal{U}_R=\frac{1}{(Z_T+\alpha_l)^3}\frac{T_+^{i\nu_P}R_-^{i\nu_T}\mathcal{T}_{+,-}}{[(\vec{A}+\vec{\tau})^2+Z_P^2]^2[(\vec{B}-\vec{\tau})^2+\alpha_k^2]^2}, \tag{2.9}$$

$$\mathcal{U}_{s_2}=(Z_T+\alpha_l)\times\frac{T_-^{i\nu_P}R_+^{i\nu_T}\mathcal{T}_{-,+}}{[(\vec{A}-\vec{\tau})^2+Z_P^2]^2[(\vec{B}+\vec{\tau})^2+\alpha_k^2]^2[\tau^2+(Z_T+\alpha_l)^2]^2}, \tag{2.10}$$

$$\mathcal{U}^{-}_{\nabla}=\frac{i\nu_P v\alpha_k}{(Z_T+\alpha_l)^3}\times\frac{T_0^{i\nu_P+1}R_0^{i\nu_T}[(1-i\nu_T)\vec{B}-i\nu_T R_0\vec{A}]\cdot(Z_P\hat{\vec{v}}+i\vec{A})}{(A^2+Z_P^2)^2(B^2+\alpha_k^2)^2}, \tag{2.11}$$

$$\mathcal{U}_{12}=\frac{1}{Z_P}\frac{(Z_T+\alpha_l)T_0^{i\nu_P}R_-^{i\nu_T}\mathcal{T}_{0,-}}{(A^2+Z_P^2)^2[(\vec{B}-\vec{\tau})^2+\alpha_k^2]^2[\tau^2+(Z_T+\alpha_l)^2]^2}, \tag{2.12}$$

$$\mathcal{U}_{x_1}=\frac{1}{2}\frac{T_0^{i\nu_P}R_0^{i\nu_T}[Z_P(1-i\nu_P)+i\nu_P(Z_P-iv)T_0]}{(A^2+Z_P^2)^2(B^2+\alpha_k^2)(Z_T+\alpha_l)^3}, \tag{2.13}$$

$$\mathcal{U}^{+}_{\nabla}=i\nu_T vZ_P\frac{T_0^{i\nu_P}R_0^{i\nu_T+1}[(1-i\nu_T)\vec{A}-i\nu_P T_0\vec{B}]\cdot(\alpha_k\hat{\vec{v}}+i\vec{B})}{(Z_T+\alpha_l)^3(A^2+Z_P^2)^2(B^2+\alpha_k^2)^2}, \tag{2.14}$$

$$\mathcal{T}_{+,-}=[Z_P(1-i\nu_P)+i\nu_P(Z_P-iv)T_+]\times[\alpha_k(1-i\nu_k)+i\nu_T(\alpha_k-iv)R_-], \tag{2.15a}$$

$$\mathcal{T}_{-,+}=[Z_P(1-i\nu_P)+i\nu_P(Z_P-iv)T_-]\times[\alpha_k(1-i\nu_k)+i\nu_T(\alpha_k-iv)R_+], \tag{2.15b}$$

$$\mathcal{T}_{0,-}=[Z_P(1-i\nu_P)+i\nu_P(Z_P-iv)T_0][\alpha_k(1-i\nu_k)+i\nu_T(\alpha_k-iv)R_-], \tag{2.15c}$$

$$T_\pm^{-1}=1+2\frac{(\vec{A}_\pm\vec{\tau})\cdot\vec{v}-iZ_Pv}{(\vec{A}\pm\vec{\tau})^2+Z_P^2},\quad T_0^{-1}=1+2\frac{\vec{A}\cdot\vec{v}-iZ_Pv}{A^2+Z_p^2}, \tag{2.16}$$

$$R_\pm^{-1}=1+2\frac{(\vec{B}\pm\vec{\tau})\cdot\vec{v}-i\alpha_k v}{(\vec{B}\pm\vec{\tau})^2+\alpha_k^2},\quad R_0^{-1}=1+2\frac{\vec{B}\cdot\vec{v}-i\alpha_k v}{B^2+\alpha_k^2}. \tag{2.17}$$

The prior $Q^{-}_{\rm if}$ and post Q^{+}_{if} total cross sections for reaction (2.1) in the CDW-4B approximation are respectively given by

TABLE I. Total cross sections (in cm^2) as a function of incident energy E (keV) for single charge exchange reaction $^4He^{2+}+{}^4He(1s^2)\rightarrow{}^4He^+(\Sigma)+{}^4He^+(1s)$. The displayed results are obtained by means of the CDW-4B approximation using the one-parameter Hylleraas wave function [labeled (a)] and the two-parameter Silverman *et al.* [29] orbitals [labeled (b)] for the initial helium bound state. The symbols $Q_{if}^{\pm}$ refer to the post (+) and prior (−) cross sections with the complete perturbation potentials according to Eqs. (2.2) and (2.3), while $Q_1^{\pm}$ represent the cross sections obtained without the term $Z_P(1/R-1/s_2)$; Q_2^+ refers to the cross section obtained without the term $(1/r_{12}-1/x_1)$ in Eq. (2.3). The numbers in the square brackets denote the powers of ten by which the numbers are to be multiplied.

E (keV)	Q_{if}^+	Q_1^+	Q_2^+	Q_{if}^-	Q_1^{-1}
100.0	(a) 1.97[−15]	1.37[−15]	1.70[−15]	2.12[−15]	1.51[−15]
	(b) 1.95[−15]	1.39[−15]	1.69[−15]	2.03[−15]	1.46[−15]
150.0	(a) 1.24[−15]	9.32[−16]	1.03[−15]	1.33[−15]	1.01[−15]
	(b) 1.18[−15]	8.95[−16]	9.80[−16]	1.21[−15]	9.30[−16]
200.0	(a) 7.83[−16]	6.19[−16]	6.35[−16]	8.36[−16]	6.67[−16]
	(b) 7.28[−16]	5.81[−16]	5.90[−16]	7.47[−16]	6.01[−16]
300.0	(a) 3.49[−16]	2.94[−16]	2.71[−16]	3.71[−16]	3.14[−16]
	(b) 3.19[−16]	2.71[−16]	2.47[−16]	3.26[−16]	2.79[−16]
400.0	(a) 1.77[−16]	1.55[−16]	1.32[−16]	1.88[−16]	1.65[−16]
	(b) 1.61[−16]	1.43[−16]	1.20[−16]	1.64[−16]	1.46[−16]
500.0	(a) 9.86[−17]	8.91[−17]	7.12[−17]	1.05[−16]	9.46[−16]
	(b) 8.94[−17]	8.22[−17]	6.42[−17]	9.14[−17]	8.42[−17]
600.0	(a) 5.90[−17]	5.45[−17]	4.13[−17]	6.26[−17]	5.78[−17]
	(b) 5.35[−17]	5.04[−17]	3.72[−17]	5.47[−17]	5.17[−17]
700.0	(a) 3.72[−17]	3.51[−17]	2.53[−17]	3.95[−17]	3.71[−17]
	(b) 3.38[−17]	3.26[−17]	2.28[−17]	3.46[−17]	3.34[−17]
800.0	(a) 2.45[−17]	2.35[−17]	1.62[−17]	2.59[−17]	2.48[−17]
	(b) 2.26[−17]	2.19[−17]	1.46[−17]	2.28[−17]	2.25[−17]
1000.0	(a) 1.17[−17]	1.15[−17]	7.39[−17]	1.24[−17]	1.21[−17]
	(b) 1.07[−17]	1.08[−17]	6.64[−18]	1.10[−17]	1.11[−17]
1500.0	(a) 2.70[−18]	2.79[−18]	1.53[−18]	2.81[−18]	2.88[−18]
	(b) 2.48[−18]	2.66[−18]	1.38[−18]	2.56[−18]	2.74[−18]
2000.0	(a) 8.67[−19]	9.24[−19]	4.50[−19]	8.87[−19]	9.36[−19]
	(b) 8.03[−19]	8.93[−19]	4.07[−19]	8.29[−19]	9.18[−19]
3000.0	(a) 1.55[−19]	1.71[−19]	6.96[−20]	1.52[−19]	1.68[−19]
	(b) 1.45[−19]	1.69[−19]	6.32[−20]	1.49[−19]	1.73[−19]
4000.0	(a) 4.21[−20]	4.79[−20]	1.70[−20]	3.99[−20]	4.53[−20]
	(b) 3.98[−20]	4.79[−20]	1.54[−20]	4.04[−20]	4.84[−20]
5000.0	(a) 1.48[−20]	1.71[−20]	5.45[−21]	1.36[−20]	1.57[−20]
	(b) 1.41[−20]	1.73[−20]	4.97[−21]	1.41[−20]	1.72[−20]
6000.0	(a) 6.13[−21]	7.18[−21]	2.11[−21]	5.47[−21]	6.43[−21]
	(b) 5.88[−21]	7.30[−21]	1.93[−21]	5.81[−21]	7.22[−21]
7000.0	(a) 2.87[−21]	3.40[−21]	9.32[−22]	2.50[−21]	2.98[−21]
	(b) 2.77[−21]	3.47[−21]	8.53[−22]	2.71[−21]	3.40[−21]
8000.0	(a) 1.48[−21]	1.76[−21]	4.56[−22]	1.26[−21]	1.51[−21]
	(b) 1.43[−21]	1.80[−21]	4.18[−22]	1.38[−21]	1.75[−21]
9000.0	(a) 8.13[−22]	9.72[−22]	2.41[−22]	6.79[−22]	8.23[−22]
	(b) 7.89[−22]	1.00[−21]	2.21[−22]	7.57[−22]	9.64[−22]
10 000	(a) 4.75[−22]	5.70[−22]	1.36[−22]	3.90[−22]	4.75[−22]
	(b) 4.62[−22]	5.89[−22]	1.25[−22]	4.39[−22]	5.62[−22]

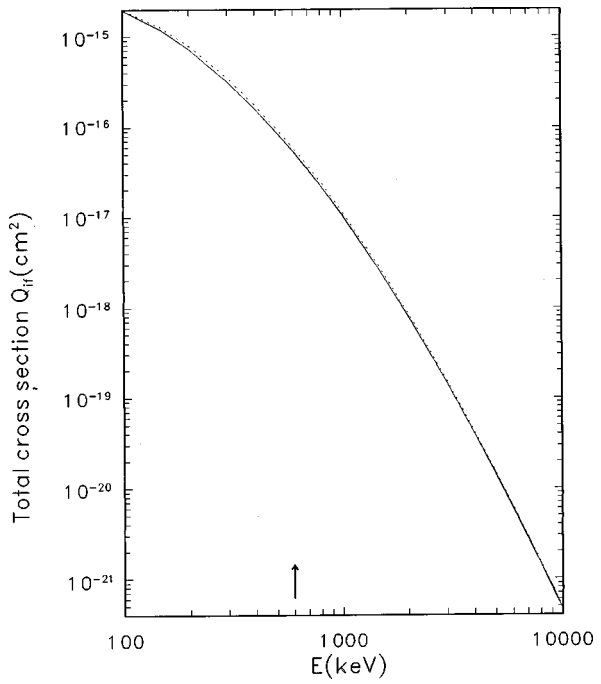

FIG. 1. Total cross sections (in cm^2) as a function of the laboratory incident energy E(keV) for the reaction $^4He^{2+}+^4He(1s^2) \rightarrow ^4He^+(\Sigma)+^4He^+(1s)$. The post cross sections of the CDW-4B model, obtained by means of the Silverman *et al.* [29] orbitals, are shown by the full line, while the dashed line represents the results obtained by the one-parameter wave function (3.1). The symbol Σ in $He^+(\Sigma)$ means that the obtained results are multiplied by 1.202 in order to include the influence of the excited state. The vertical arrow indicates the lower limit of application of the CDW-4B theory.

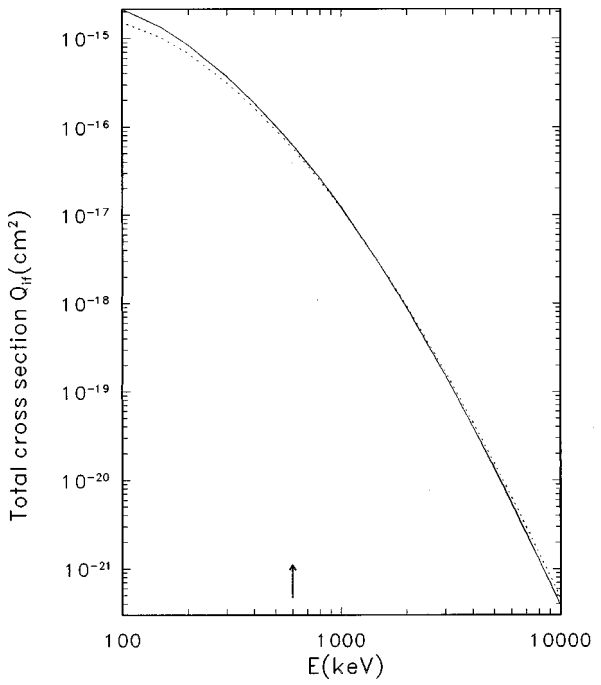

FIG. 2. Same as in Fig. 1 except that the full and dashed curves correspond to the prior total cross sections obtained with the full perturbation potential, and with the neglected term $Z_P(1/R - 1/s_2)$, respectively. The ground state of the target atom $He(1s^2)$ is described by means of the wave function (3.1).

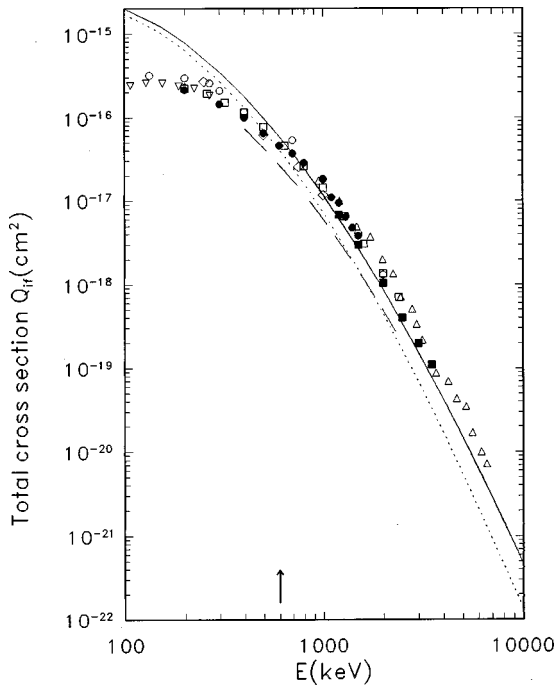

FIG. 3. Total cross sections (in cm^2) as a function of the laboratory incident energy E(keV) for the reaction $^4He^{2+}+^4He(1s^2) \rightarrow ^4He^+(\Sigma)+^4He^+(1s)$. The full and dashed lines represent the post cross section Q_{if}^+ of the CDW-4B approximation with the complete perturbation potential and without the potential $(1/r_{12}-1/x_1)$, respectively. The displayed CDW-4B results are obtained by means of the wave function (3.1) for the ground state of the helium target atom. The long-dashed curve refers to the theoretical CDW results of Dunseath and Crothers [9], derived by using the Pluvinage wave function with the corresponding theoretical binding energy. Experimental data: ○, DuBois [30]; ▽, Shah *et al.* [31]; ◇, Mergel *et al.* [32]; ●, Shah and Gilbody [33]; □, Pivovar *et al.* [34]; △, Hvelplund *et al.* [35]; ■, de Castro Faria *et al.* [36].

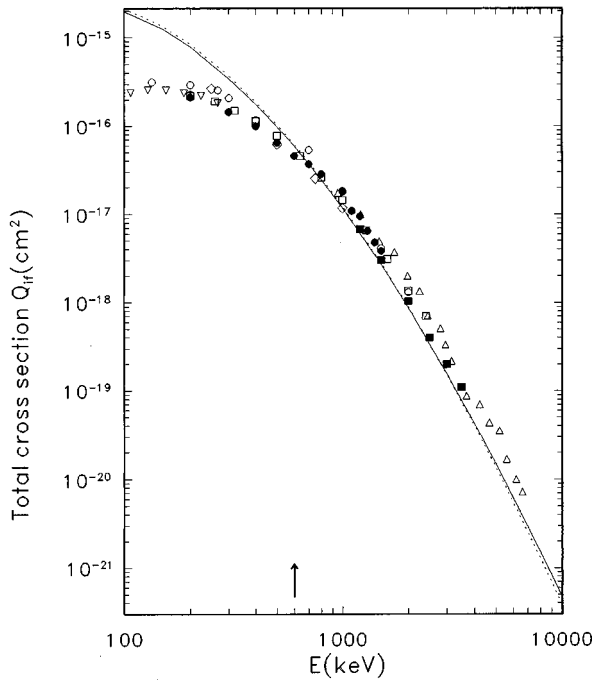

FIG. 4. Same as in Fig. 3 except that the full and dashed curves represent the post and prior total cross sections, respectively.

TABLE II. Same as in Table I except for the reaction $p+{}^7\mathrm{Li}^+(1s^2)\rightarrow H(\Sigma)+{}^7\mathrm{Li}^{2+}(1s)$.

E (keV)	Q_{if}^+	Q_1^+	Q_2^+	Q_{if}^-	Q_1^{-1}
50.0	(a) 1.84[−17]	2.19[−17]	2.49[−17]	2.18[−17]	2.43[−17]
	(b) 1.83[−17]	2.18[−17]	2.41[−17]	1.80[−17]	2.14[−17]
60.0	(a) 1.81[−17]	1.89[−17]	2.55[−17]	2.05[−17]	2.08[−17]
	(b) 1.80[−17]	1.88[−17]	2.50[−17]	1.77[−17]	1.85[−17]
70.0	(a) 1.71[−17]	1.70[−17]	2.37[−17]	1.87[−17]	1.83[−17]
	(b) 1.70[−17]	1.69[−17]	2.34[−17]	1.68[−17]	1.67[−17]
80.0	(a) 1.56[−17]	1.52[−17]	2.10[−17]	1.66[−17]	1.61[−17]
	(b) 1.55[−17]	1.51[−17]	2.08[−17]	1.54[−17]	1.50[−17]
90.0	(a) 1.39[−17]	1.35[−17]	1.82[−17]	1.46[−17]	1.41[−17]
	(b) 1.38[−17]	1.34[−17]	1.81[−17]	1.37[−17]	1.33[−17]
100.0	(a) 1.23[−17]	1.19[−17]	1.56[−17]	1.27[−17]	1.23[−17]
	(b) 1.22[−17]	1.18[−17]	1.55[−17]	1.21[−17]	1.17[−17]
150.0	(a) 6.25[−18]	6.10[−18]	7.17[−18]	6.30[−18]	6.16[−18]
	(b) 6.12[−18]	6.01[−18]	7.04[−18]	6.12[−18]	6.00[−18]
200.0	(a) 3.27[−18]	3.23[−18]	3.51[−18]	3.28[−18]	3.24[−18]
	(b) 3.16[−18]	3.14[−18]	3.40[−18]	3.16[−18]	3.14[−18]
300.0	(a) 1.06[−18]	1.06[−18]	1.04[−18]	1.07[−18]	1.07[−17]
	(b) 1.00[−18]	1.02[−18]	9.86[−19]	1.00[−18]	1.01[−18]
400.0	(a) 4.14[−19]	4.18[−19]	3.83[−19]	4.20[−19]	4.25[−19]
	(b) 3.88[−19]	3.98[−19]	3.58[−19]	3.86[−19]	3.96[−19]
500.0	(a) 1.85[−19]	1.88[−19]	1.63[−19]	1.89[−19]	1.92[−19]
	(b) 1.73[−19]	1.79[−19]	1.52[−19]	1.72[−19]	1.79[−19]
600.0	(a) 9.16[−20]	9.39[−20]	7.79[−20]	9.41[−20]	9.64[−20]
	(b) 8.57[−20]	8.94[−20]	7.24[−20]	8.57[−20]	8.95[−20]
700.0	(a) 4.92[−20]	5.07[−20]	4.04[−20]	5.06[−20]	5.21[−20]
	(b) 4.61[−20]	4.84[−20]	3.76[−20]	4.62[−20]	4.86[−20]
800.0	(a) 2.81[−20]	2.91[−20]	2.25[−20]	2.90[−20]	2.99[−20]
	(b) 2.64[−20]	2.79[−20]	2.09[−20]	2.66[−20]	2.81[−20]
900.0	(a) 1.69[−20]	1.76[−20]	1.32[−20]	1.74[−20]	1.81[−20]
	(b) 1.59[−20]	1.69[−20]	1.23[−20]	1.61[−20]	1.71[−20]
1000.0	(a) 1.06[−20]	1.11[−20]	8.08[−21]	1.09[−20]	1.14[−20]
	(b) 1.00[−20]	1.07[−20]	7.55[−21]	1.02[−21]	1.08[−20]
1500.0	(a) 1.64[−21]	1.73[−21]	1.13[−21]	1.66[−21]	1.75[−21]
	(b) 1.57[−21]	1.70[−21]	1.07[−21]	1.60[−21]	1.73[−21]

$$Q_{if}^{\pm}(a_0^2)=\int d\vec{\eta}\left|\frac{R_{if}^{\pm}(\vec{\eta})}{2\pi v}\right|^2. \tag{2.18}$$

The integration over ϕ_η can be calculated analytically with the results 2π, due to the axial symmetry of the integrand, while the quadrature over η has to be performed numerically. Hence, the total cross sections $Q_{if}^{\pm}$ in the CDW-4B theory for single charge exchange can be reduced to a four-dimensional numerical quadrature.

III. RESULTS AND DISCUSSION

Numerical computations are performed describing the initial heliumlike ground state by means of the one-parameter Hylleraas orbital,

$$\varphi_i(\vec{x}_1,\vec{x}_2)=\frac{\alpha^3}{\pi}e^{-\alpha(x_1+x_2)}, \tag{3.1}$$

and the CI wave function $(1s1s')$ of Ref. [29] with the radial static correlations,

$$\varphi_i(\vec{x}_1,\vec{x}_2)=\frac{N}{\pi}(e^{-\alpha_1 x_1-\alpha_2 x_2}+e^{-\alpha_2 x_1-\alpha_1 x_2}),$$
$$N=\left[\frac{1}{\alpha_1^3}+\frac{1}{\alpha_2^3}+\frac{16}{(\alpha_1+\alpha_2)^3}\right]^{-1/2}. \tag{3.2}$$

The explicit computations of the total cross sections are carried out only for the final ground states $f_1=1s$ and $f_2=1s$. The obtained results are multiplied additionally by a factor of 1.202 in order to include a contribution from the excited states according to the n^{-3} Oppenheimer scaling law. First, we shall consider the symmetric charge-changing reaction (1.1). The results of the computations of the post and prior total cross sections at energies 100–10 000 keV are summarized in Table I and Figs. 1–4. The columns headed by the symbols Q_{if}^+ and Q_{if}^- represent the post and prior cross sections obtained with the complete perturbations according to Eqs. (2.2) and (2.3). In order to examine the relative role of the various terms in these perturbations, we have

computed total cross sections by (i) neglecting the term $Z_P(1/R-1/s_2)$ in the post and prior version; these results in Table I are labeled as Q_1^+ and Q_1^-, respectively, and (ii) neglecting the term $(1/r_{12}-1/x_1)$ in the post transition amplitude; the corresponding findings are denoted by Q_2^+. The total cross sections obtained by means of the wave functions (3.1) are labeled (a) in Table I, while the results denoted by (b) are derived using the two-parameter orbitals of Ref. [29].

The total cross sections obtained with the Hylleraas wave function (3.1) and the radially correlated orbitals of Ref. [29] are very close to each other, as can be seen in Fig. 1, where we have compared the post total cross sections for these functions. The radial correlations in the wave function of Ref. [29] are taken into account to within nearly 95%. Although the Hylleraas wave function is less accurate, it includes some form of the radial correlations through the presence of the Slater-screened effective charge of the target nucleus. Further, the prior form (2.2) does not contain the term $1/r_{12}$, which explicitly accounts for the dynamical correlations. As a result, the prior amplitude and, therefore, the prior cross sections, are more sensitive to the accuracy of the initial state than the corresponding results form the post form (2.3). This is verified in Table I by comparing the values of Q_{if}^+ and Q_{if}^- computed with Hylleraas' and Silverman *et al.* [29] wave functions. The effect is less important for the Li^+ target due to a higher nuclear charge (see Table II).

When in the prior form we neglect the term $Z_P(1/R-1/s_2)$, we have readily reproduced the results of Refs. [4,5,6] for capture to the ground state for functions (3.1) and (3.2). In Fig. 2 the prior total cross sections with the complete perturbation potential are shown together with the results obtained only with the scalar product of the gradient operators, i.e., the cross sections derived by ignoring the term $Z_P(1/R-1/s_2)$. The difference between the two curves does not exceed 15% above 30 keV/amu. The term $Z_P(1/R-1/s_2)$ also has a similar influence on the results obtained in the case of the post formalism, which can be observed from Table I. The potential $-Z_P/s_2$ has the asymptotic value $-Z_P/R$ at large distances between Z_P and e_2. A relatively small contribution of the term $Z_P(1/R-1/s_2)$ suggests that, for single electron capture at intermediate and high energies, the potential $-Z_P/s_2$ is nearly cancelled by $-Z_P/R$. Therefore, in a rougher computation this term can be ignored.

The post total cross sections derived with the full perturbation according to Eq. (2.3), as well as without the term $(1/r_{12}-1/x_1)$, are displayed in Fig. 3, where a number of experimental data are also plotted. Our CDW-4B approximation with the complete perturbation (the full line in Fig. 3) is in good agreement with the available measurements above 150 keV/amu. We recall that the lower limit of application of the CDW-3B theory has been established in Ref. [3]. When we neglect the relevant term for the dynamic electron correlation $(1/r_{12}-1/x_1)$ from Eq. (2.3), we have obtained the results (the dashed curve in Fig. 3) that underestimate the experimental findings. The difference between the two curves becomes more significant at higher impact energies. This means that the dynamic electron correlations play a very important role, especially at higher impact energies. A similar conclusion has been previously reached in Ref. [17] for single electron capture in the p-He collision, as well as

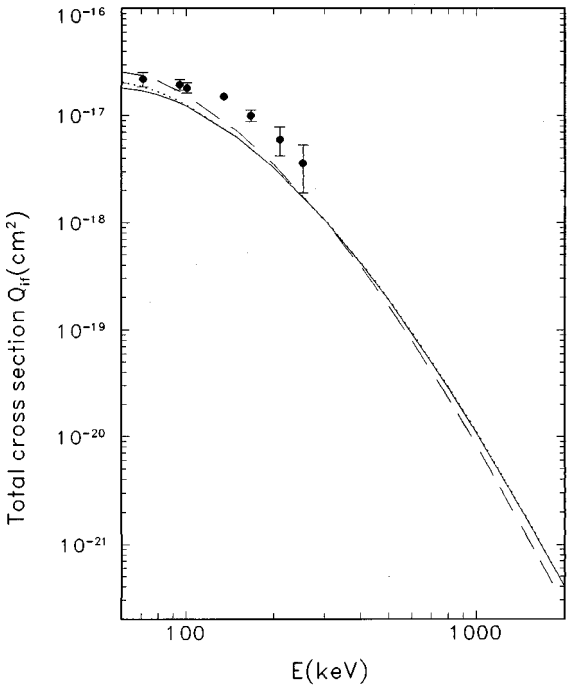

FIG. 5. Total cross sections (in cm^2) as a function of the laboratory incident energy E(keV) for the reaction: $p+{}^7Li^+(1s^2) \rightarrow H(\Sigma)+{}^7Li^{2+}(1s)$. The full and the dashed lines respectively represent the post Q_{if}^+ and prior Q_{if}^- cross sections of the CDW-4B approximation with the complete perturbation potentials. The long-dashed curve refers to the theoretical CDW-4B results obtained without the term $(1/r_{12}-1/x_1)$ in Eq. (2.3). Experimental data: ●, Sewell *et al.* [27].

for the transfer ionization [16] in α-He scattering. In the same figure, a comparison is made between our CDW-4B theory and the CDW method of Ref. [9], derived using the Pluvinage wave function with the corresponding theoretical binding energies. Their method ignores the dynamic correlations and this may be one of the reasons for a less favorable agreement with the experimental data. On the other hand, this indicates that the dynamic electronic correlations in the active perturbation potentials are more important than the static ones in the target bound-state wave function. The exact wave function for He$(1s^2)$ is unavailable at present and this leads to the so-called post-prior discrepancy in the cross sections. Further, the discrepancy between the post and prior cross sections depends essentially on the level of approximation made to determine the ground-state wave function of helium. This discrepancy is greater in the case of the Hylleraas wave function than the Silverman *et al.* orbital [29]. For the former case, it does not exceed 20% (see Table I and Fig. 4) for the α-He collision in the considered energy interval, while for the Silverman *et al.* function [29], it is in the range up to 5% (see Table I). For instance, at impact energies 600, 6000, and 10 000 keV, the post-prior discrepancy for the Hylleraas wave function is 6.2%, 10.8%, and 17.9%, respectively, while at the same energies for the Silverman *et al.* orbital [29], it is 2.2%, 1.2%, and 4.9%, respectively. The post-prior discrepancy would not exist if an exact wave function was utilized.

The obtained theoretical results for reaction (1.2) are plotted in Fig. 5. Our total cross sections are compared with the

experimental findings of Ref. [27]. Unfortunately, their measurements are limited up to 250 keV. As can be seen, our theoretical results slightly underestimate these experimental data. The CDW-4B model is a high-energy approximation and we expect better agreement at larger impact energies. New measurements for the considered reaction are needed for a better assessment of the validity of the CDW-4B theory. We note that there is good agreement between our results and the POHCE calculation of Ref. [24]. The CTMC results show a different trend. Namely, this cross section shows a peak around 175 keV; this is not seen in our calculation nor in the experimental data or the in POHCE method of Ref. [24].

IV. CONCLUSION

We have investigated the problem of single-electron capture in the α-He and p-Li^+ collisions at intermediate and high impact energies. The four-body continuum distorted wave (CDW-4B) methods is used for computing the post and prior total cross sections. In this formalism, both the static and dynamic electron correlations are automatically included through the perturbation potentials and/or via the bound state wave function. The relative importance of the various terms in the perturbation potentials is evaluated. The obtained results indicate that the dynamic electron correlations are very important, especially at higher impact energies. Comparisons between the present theoretical cross sections and a number of experimental data in the α-He collision yield good agreement at impact energies $E \geqslant 150$ keV/amu, while in the p-Li^+ scattering, our results slightly underestimate the available experimental data, which are limited up to 250 keV. New measurements covering higher energies are necessary for this reaction.

ACKNOWLEDGMENT

Thanks are due to Professor Dževad Belkić for helpful discussions and a critical review of the manuscript.

[1] I. M. Cheshire, Proc. Phys. Soc. London **84**, 89 (1964).
[2] R. Gayet, J. Phys. B **5**, 483 (1972).
[3] Dž. Belkić, R. Gayet, and A. Salin, Phys. Rep. **56**, 279 (1979).
[4] Dž. Belkić and R. Janev, J. Phys. B **6**, 1020 (1973).
[5] Dž. Belkić and R. Gayet, J. Phys. B **10**, 1923 (1977).
[6] R. Gayet, R. D. Rivarola, and A. Salin, J. Phys. B **14**, 2421 (1981).
[7] R. Gayet and A. Salin, J. Phys. B **20**, L571 (1987).
[8] D. S. Crothers and R. McCarroll, J. Phys. B **20**, 2835 (1987).
[9] K. M. Dunseath and D. S. Crothers, J. Phys. B **24**, 5003 (1991).
[10] Dž. Belkić and I. Mančev, Phys. Scr. **45**, 35 (1992).
[11] Dž. Belkić and I. Mančev, Phys. Scr. **47**, 18 (1993).
[12] R. Gayet, J. Hanssen, L. Jacqui, A. Martinez, and R. Rivarola, Phys. Scr. **53**, 549 (1996).
[13] R. Gayet and J. Hanssen, J. Phys. B **25**, 825 (1992).
[14] H. Bachau, R. Gayet, J. Hanssen and A. Zerarka, J. Phys. B **25**, 839 (1992).
[15] R. Gayet, J. Hanssen, and L. Jacqui, J. Phys. B **28**, 2193 (1995).
[16] Dž. Belkić, I. Mančev, and V. Mergel, Phys. Rev. A **55**, 378 (1997).
[17] Dž. Belkić, R. Gayet, J. Hanssen, I. Mančev, and A. Nuñez, Phys. Rev. A **56**, 3675 (1997).
[18] Dž. Belkić, Phys. Scr. **40**, 610 (1989).
[19] V. A. Sidorovich, V. S. Nikolaev, and J. H. McGuire, Phys. Rev. A **31**, 2193 (1985).
[20] T. C. Theisen and J. H. McGuire, Phys. Rev. A **20**, 1406 (1979).
[21] R. H. Bassel and E. Gerjuoy, Phys. Rev. **113**, 749 (1960).
[22] R. Shingal and C. D. Lin, J. Phys. B **24**, 251 (1991).
[23] A. E. Wetmore and R. E. Olson, Phys. Rev. A **38**, 5563 (1988).
[24] A. L. Ford, J. F. Reading, and R. L. Becker, J. Phys. B **15**, 3257 (1982).
[25] Yu. R. Kuang, J. Phys. B **24**, 1645 (1991).
[26] R. E. Olson and A. Salop, Phys. Rev. A **16**, 531 (1977).
[27] E. C. Sewell, G. C. Angel, K. F. Dunn, and H. B. Gilbody, J. Phys. B **13**, 2269 (1980).
[28] G. W. Shirtcliffe and K. E. Banyard, Phys. Rev. A **21**, 1197 (1980); J. Phys. B **12**, 3247 (1979).
[29] J. N. Silverman, O. Platas, and F. A. Matsen, J. Chem. Phys. **32**, 1402 (1960).
[30] R. D. DuBois, Phys. Rev. A **36**, 2585 (1987).
[31] M. B. Shah, P. McCallion, and H. B. Gilbody, J. Phys. B **22**, 3037 (1989).
[32] V. Mergel, R. Dörner, O. Jagutzki, S. Leneinas, S. Nüttgens, L. Spielberger, M. Unverzagt, C. L. Cocke, R. E. Olson, M. Schultz, U. Buck, E. Zanger, W. Theisinger, M. Isser, S. Geis, and H. Schmidt-Böcking, Phys. Rev. Lett. **74**, 2200 (1995).
[33] M. B. Shah and H. B. Gilbody, J. Phys. B **18**, 899 (1985).
[34] L. I. Pivovar, V. M. Tabaev, and M. T. Nikolov, Zh. Eksp. Teor. Fiz. **41**, 26 (1961) [Sov. Phys. JETP **14**, 20 (1962)].
[35] P. Hvelplund, J. Heinemei, E. Horsdal-Pedersen, and F. R. Simpson, J. Phys. B **9**, 491 (1976).
[36] N. V. de Castro Faria, F. L. Freire, and A. G. Pinho, Phys. Rev. A **37**, 280 (1988).